Title
Targeted expression of a lumican transgene rescues corneal deficiencies in lumican-null mice.

Journal
Molecular vision, 13

ISSN
1090-0535

Authors
Meij, Johanna T A
Carlson, Eric C
Wang, Li
et al.

Publication Date
2007-10-18

Peer reviewed

Molecular Vision 2007; 13:2012-8 <http://www.molvis.org/molvis/v13/a226/>
Received 27 August 2007 | Accepted 18 October 2007 | Published 18 October 2007

Targeted expression of a lumican transgene rescues corneal deficiencies in lumican-null mice

Johanna T.A. Meij,[1] Eric C. Carlson,[1] Li Wang,[1] Chia-Yang Liu,[1] James V. Jester,[3] David E. Birk,[4] Winston W.Y. Kao[1,2]

Departments of [1]Ophthalmology, and [2]Cell and Cancer Biology, University of Cincinnati, Cincinnati, OH; [3]The Eye Institute, University of California, Irvine, CA; [4]Department of Pathology, Anatomy & Cell Biology, Thomas Jefferson University, Philadelphia, PA

Purpose: To investigate whether targeted expression of lumican in the mouse cornea rescued the *Lum*$^{-/-}$ phenotype.
Methods: *Lum*$^{-/-}$/*Kera-Lum* mice were generated by crossing *Lum*$^{-/-}$ mice with *Kera-Lum* transgenic mice that overexpressed lumican under the control of the keratocan promoter. Mouse eyes were analyzed in vivo by confocal microscopy through focusing (CMTF) to determine corneal sublayer thickness and haze. Subsequently, one cornea from each mouse was processed for SDS-PAGE/western blotting while the other was used for either electron microscopy (EM) or real-time polymerase chain reaction (RT-PCR).
Results: Overall, corneas of *Lum*$^{-/-}$/*Kera-Lum* mice showed significant improvement over *Lum*$^{-/-}$ but were still deficient when compared to wildtype (WT) mice. Specifically, analysis of *Lum*$^{-/-}$/*Kera-Lum* mouse eyes by CMTF showed a similar stromal but slightly increased epithelial thickness compared to matching *Lum*$^{-/-}$ mice. Analysis of the CMTF scans for light backscattering revealed a small yet significant reduction in corneal haze in *Lum*$^{-/-}$/*Kera-Lum* mice as compared to *Lum*$^{-/-}$ mice. At the EM level, the pronounced disarray of the posterior fibrillar matrix seen in *Lum*$^{-/-}$ mice was not observed in *Lum*$^{-/-}$/*Kera-Lum* mice. Moreover, analyses of collagen fibril diameter distributions showed a significant reduction in the number of large-diameter (>40 nm) fibrils in *Lum*$^{-/-}$/*Kera-Lum* mice as compared to *Lum*$^{-/-}$ mice. No significant differences in keratocan expression were found at the mRNA level, but western blot analysis detected an approximately two fold increase in keratocan protein levels in *Lum*$^{-/-}$/*Kera-Lum* over *Lum*$^{-/-}$ mice.
Conclusions: Together these data suggest that despite the low keratocan promoter activity driving the transgene in *Lum*$^{-/-}$ cornea, transgenic lumican expression was sufficient to partially rescue corneal phenotypic deficiencies.

The vertebrate cornea is a transparent and avascular tissue that covers the anterior chamber of the eye and provides most of the eye's refractive power. It consists of three functionally and structurally different cellular layers, the corneal epithelium, stroma, and endothelium. The mechanical and optical properties of the cornea are determined by its extracellular matrix (ECM) organization such as collagens and proteoglycans in the stroma. The stromal ECM is abundant in collagen fibrils and two small class II leucine-rich proteoglycans, lumican and keratocan, which are synthesized and deposited by stromal keratocytes [1]. The functional importance of these keratan sulfate proteoglycans for corneal structure is most evident in knockout mouse lines. Mice lacking the gene for keratocan display a thinner and flatter but functionally normal cornea [2]. Mice deficient in lumican (*Lum*$^{-/-}$) have a disorganized corneal posterior stroma, characterized by the presence of thickened and irregular collagen fibrils [3-5]. As a consequence, corneal transparency is dramatically reduced. In addition, *Lum*$^{-/-}$ mice have reduced corneal keratocan levels, consistent with the finding that lumican regulates keratocan transcription [6].

Unlike keratocan, lumican is present in a wide range of connective tissues. Lumican-null mice exhibit a phenotype that includes severe skin fragility as well as cloudy corneas [3-5,7]. Therefore, it remains to be determined whether the corneal deficiencies in *Lum*$^{-/-}$ mice result solely from a cornea-intrinsic defect or also from a systemic defect. In the present study, we investigated whether corneal reexpression of lumican in a *Lum*$^{-/-}$ background rescued the phenotypic deficits. To this end, *Kera-Lum* transgenic mice carrying a minigene with lumican cDNA under the control of the 3.2 kb keratocan promoter [6] were crossed with *Lum*$^{-/-}$ mice [3] to generate *Lum*$^{-/-}$/*Kera-Lum* mice. Our findings show a significant improvement of corneal properties in *Lum*$^{-/-}$/*Kera-Lum* as compared to *Lum*$^{-/-}$ mice, indicating that reexpression of corneal lumican in a lumican-null background is able to rescue phenotypic deficits.

METHODS

Animals: Animal care and use conformed to the ARVO Statement for the Use of Animals in Ophthalmic and Vision Research. All animal protocols were approved by the Institutional Animal Care and Use Committee (IACUC) of the University

Correspondence to: Winston W.Y. Kao, Ph.D., 3223 Eden Ave, HPB Suite 350, Cincinnati, OH, 45267-0838; Phone: (513) 558-2802; FAX: (513) 558-6021; email: kaoww@uc.edu

Dr. Carlson is now at the Department of Ophthalmology and Pathology, Visual Science Research Center, Case Western Reserve University, Cleveland, OH.

of Cincinnati. *Lum*$^{-/-}$ mice [3] of a mixed J129/B6 background strain were cross-bred with *Kera-Lum* transgenic mice (FVB/B6) that overexpressed lumican under control of the keratocan promoter [6]. After genotyping, the bitransgenic *Lum*$^{-/-}$/*Kera-Lum* mice from one line were used in this study and compared to age-matched and strain-matched *Lum*$^{-/-}$ mice.

In vivo confocal microscopy: In vivo confocal microscopy through focusing (CMTF) was used to measure corneal epithelial thickness, stromal thickness, and stromal light scattering. Mice were anesthetized by intraperitoneal injection of ketamine HCl (100 mg/kg body weight; Dodge Animal Health, Fort Dodge, IA) and xylazine (10 mg/kg body weight; Akorn Inc., Decatur, IL), and the central cornea was scanned using a tandem scanning confocal microscope (Tandem Scanning Corp., Reston, VA). Thickness and light scattering measurements were obtained using previously described techniques [8-10]. Three confocal microscopy through focus (CMTF) scans, each comprised of a sequential series of 200 images extending from the corneal epithelial surface through the corneal endothelium, were obtained from each mouse eye. Depth intensity profiles were generated, and thickness measurements for the epithelium and stroma as well as stromal light scattering were obtained using previously published equations [9-11]. An average of the epithelial thickness, stromal thickness, and stromal light scattering from the three separate z-scans taken from the same eye were recorded. The value per mouse was calculated from the average of both eyes and used for statistical analysis. After in vivo confocal microscopy, mice were sacrificed and the eyes enucleated and either immediately frozen for biochemical analysis or fixed for electron microscopy.

Transmission electron microscopy: Corneas from three to four mice per group were analyzed by transmission electron microscopy. The corneas were processed as previously described [4,12]. Briefly, fixation was with 4% paraformaldehyde, 2.5% glutaraldehyde, 0.1 M sodium cacodylate, pH 7.4, and 8.0 mM $CaCl_2$ followed by postfixation with 1% osmium tetraoxide and *en bloc* stained with uranyl acetate/50% ethanol. After dehydration in an ethanol series followed by propylene oxide, the corneas were infiltrated and embedded in a mixture of EMbed 812, nadic methyl anhydride, dodecenyl succinic anhydride, and DMP-30 (Electron Microscopy Sciences, Hatfield, PA). Thin sections were cut using a Reichert UCT ultramicrotome equipped with a diamond knife and stained with 2% aqueous uranyl acetate, 1% phosphotungstic acid, pH 3.2. Sections taken from the central cornea and the anterior and posterior stroma were analyzed independently using electron microscopy. Corneas were examined and photographed at 80 kV using a Tecnai 12 transmission electron microscope with a Gatan 2K Ultrascan bottom mount CCD camera.

Fibril diameter analyses: Corneas from two to three different animals were analyzed for each transgenic line. Digital images were taken from nonoverlapping regions of the central portion of anterior and posterior areas of the cornea at 28,610X. Images (10-15 anterior and 15-20 posterior/group) were randomized and fibril diameters were measured using a RM Biometrics-Bioquant Image Analysis System (Nashville,TN) in a masked manner. A total area of 0.211 μm^2 per image at a final magnification of 161,990X was analyzed. For each group, the number of animals and number of different images (animals/images [fibril count, min-max diameter]) was as follows: wildtype (WT) anterior (3/15 [2,379, 8.2 - 41.9 nm]); WT posterior (3/15 [1,893, 8.2 - 43.2 nm]); *Lum*$^{-/-}$ anterior (2/10 [1,496, 8.2 - 38.7 nm]); *Lum*$^{-/-}$ posterior (3/15 [1,815, 5.8 - 59.9 nm]); *Lum*$^{-/-}$/*Kera-Lum* anterior (3/15 [2,135, 9.2 - 50.0 nm]); *Lum*$^{-/-}$/*Kera-Lum* posterior (4/20 [2,224, 5.8 - 51.4 nm]). The smallest diameter measurements (5-9 nm) represent the tapered ends of corneal collagen fibrils near their termination [12-14]. Although the corneal stroma also contains fibrillin-containing microfibrils in this diameter range, those have a distinctive structure and organization and were excluded from the measurements.

Real-time polymerase chain reaction: Corneas were excised from frozen eyes of a subset of animals (11 *Lum*$^{-/-}$ and 10 *Lum*$^{-/-}$/*Kera-Lum*), and RNA was prepared using the FastRNA Pro Green kit (QBiogene, Morgan Irvine, CA). Briefly, each cornea was placed in 0.8 ml RNA*pro* solution and homogenized with Lysing Matrix D in a Fastprep instrument (QBiogene) at setting 6.0 for 40 s. After cooling on ice, supernatants were transferred and the lysing matrices rinsed with 0.2 ml RNA*pro* solution. Combined supernatants were chloroform-extracted, and RNA was precipitated from the upper phase with an equal volume of isopropanol overnight at -20 °C. Pellets were rinsed with 70% ethanol, air-dried, and resuspended in 10 μl/cornea DEPC-treated H_2O at 55-60 °C for 10 min. RNA quality was checked by agarose gel electrophoresis.

To obtain cDNA, RNA was reverse-transcribed using a RETROScript kit with random primers (Ambion, Austin, TX). Real-time polymerase chain reaction (RT-PCR) was performed on a SmartCycler system (Cepheid, Sunnyvale, CA) using β-actin as the reference gene. The primer pairs were as follows: Keratocan: Kerac-F2: 5'-AAT GCT AAC CTG CAG CAC CTT CAC-3' and Kerac-R2: 5'-TTC ATT CCC ATC CAG ACG CAG GTA-3'; β-actin: bact-F1: 5'-TGG CTC CTA GCA CCA TGA AGA TCA-3' and bact-R2: 5'-ACT CAT CGT ACT CCT GCT TGC TGA-3'. For the reaction mix, a LightCycler DNA Master SYBR Green I kit (Roche Applied Science, Indianapolis, IN) was employed. Optimum conditions were determined by PCR using the kit components and agarose gel analysis. Also, a cDNA dilution series was run to determine the RT-PCR efficiency of each primer pair. One *Lum*$^{-/-}$ sample was randomly chosen as the "control" and included in all subsequent runs. Crossing point differences between samples and the "control" and the calculated efficiencies were applied to compute the expression ratio of keratocan in the corneal extracts according to the formula by Pfaffl [15].

SDS-PAGE/western blotting: Corneas were excised from frozen eyes and solubilized in 50 mM Tris-NaOH, pH 12.0, containing 0.25 U/μl Benzonase nuclease (Novagen, Madison, WI) and protease inhibitor cocktail (Roche Applied Science, Indianapolis, IN), overnight at 4 °C in a rotator [16]. The samples were centrifuged at 14,000x g for 15 min, and

the collected supernatants were neutralized with 1/10 volume of 500 mM Tris-HCl, pH 6.0. To estimate protein concentration, absorbance was measured with a spectrophotometer at 280 nm. Extracts were digested with 0.1 U/ml endo-β-galactosidase (Sigma, St Louis, MO) at 37 °C overnight, and the reaction was terminated by the addition of 1 vol 2x SDS-PAGE sample buffer. SDS-PAGE and western blotting were performed as described previously [16], using goat anti-Keratocan [2] as the primary antibody and IRDye 800-conjugated donkey anti-goat IgG (Rockland Immunochemicals, Gilbertsville, PA) as the secondary antibody. Immunopositive bands were quantified with an Odyssey Infrared Imaging system (LI-COR Biosciences, Lincoln, NE). One *Lum*$^{-/-}$/*Kera-Lum* sample was chosen for normalization and included in all assays.

Statistical analysis: Data were analyzed using GraphPad Prism version 5.00 for Windows (GraphPad Software, San Diego, CA). Data were compared by either ANOVA followed by Newman-Keuls Multiple Comparison Test or *t*-test with Welch's correction for unequal variances where stated. Differences were considered significant when $p<0.05$.

RESULTS

Absence of lumican in the mouse cornea causes corneal thinning and severe opacity associated with disorganization of and aberrations in collagen fibrils most prominently in the poste-

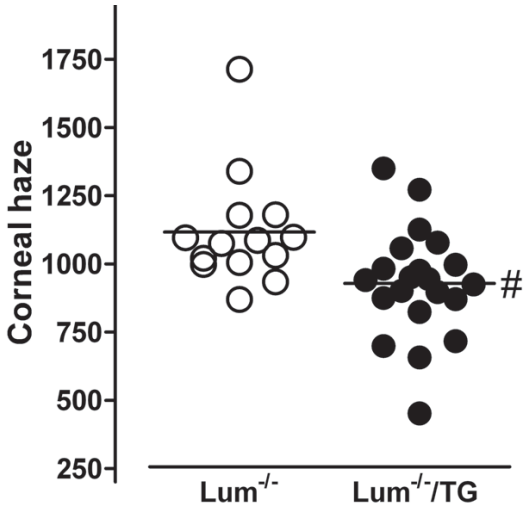

Figure 2. Corneal haze in *Lum*$^{-/-}$ and *Lum*$^{-/-}$/*Kera-Lum* (*Lum*$^{-/-}$/TG) mice. The same CMTF scans as used for Figure 1 were analyzed for stromal light scattering as described in Methods. Symbols represent the average of six scans (three per eye) per individual *Lum*$^{-/-}$ mouse (open symbol) and *Lum*$^{-/-}$/*Kera-Lum* mouse (closed symbol). Horizontal lines respresent the mean values per group: 1,116±55.2 nm, *Lum*$^{-/-}$; 927.6±43.7 nm, *Lum*$^{-/-}$/*Kera-Lum*; 489.1±28.6 nm, WT (not shown). The hash mark indicates significance ($p<0.02$) versus *Lum*$^{-/-}$ (*t*-test with Welch's correction).

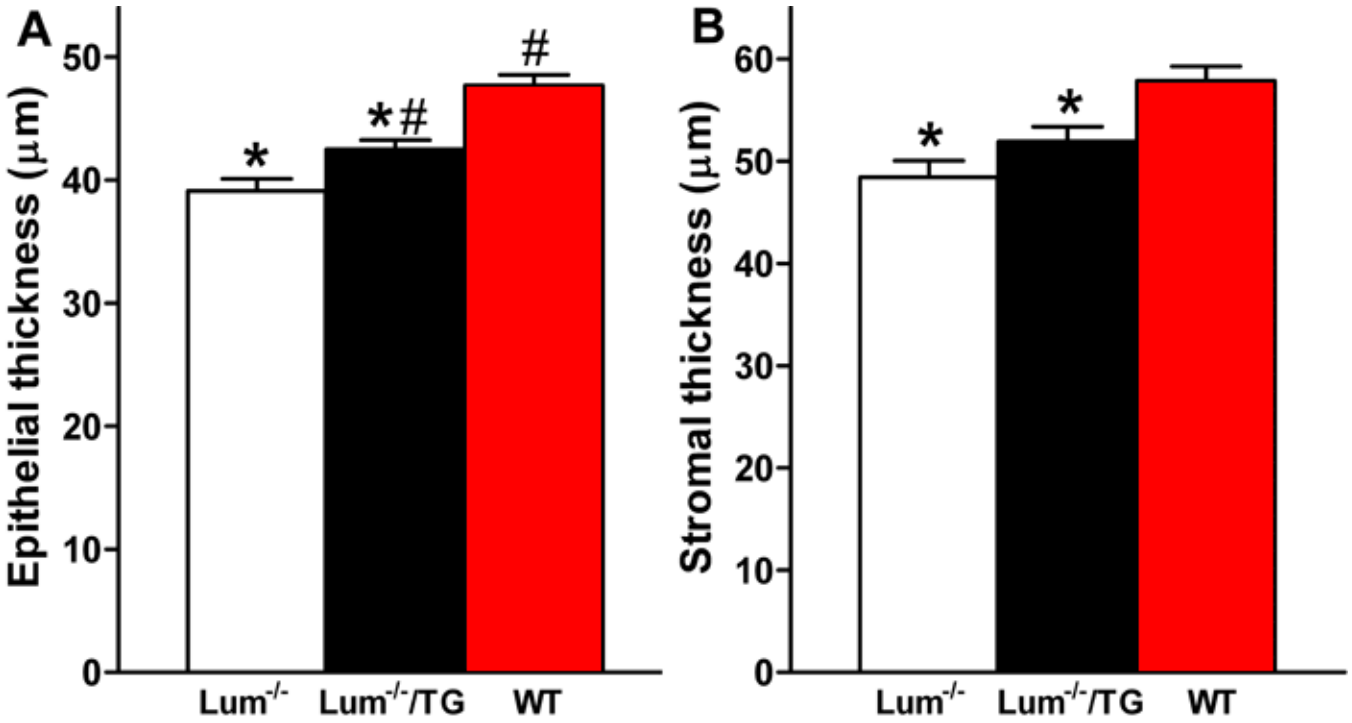

Figure 1. Corneal thickness in *Lum*$^{-/-}$, *Lum*$^{-/-}$/*Kera-Lum* (Lum$^{-/-}$/TG), and WT mice. Thickness of corneal epithelial (**A**) and stromal (**B**) layers in *Lum*$^{-/-}$, *Lum*$^{-/-}$/*Kera-Lum* (Lum$^{-/-}$/TG), and WT mice are shown. Mice were anesthetized and the central corneas were scanned by confocal microscopy through focusing (CMTF) as described in Methods. Data represent the mean±SEM of six scans per mouse (three per eye) of 14 *Lum*$^{-/-}$, 21 *Lum*$^{-/-}$/*Kera-Lum*, and seven WT mice. Reexpression of lumican in *Lum*$^{-/-}$ partially rescued the epithelial thickness in comparison to WT and *Lum*$^{-/-}$/*Kera-Lum* versus *Lum*$^{-/-}$; however, no significant improvement of stromal thickness could be determined comparing *Lum*$^{-/-}$/*Kera-Lum* to *Lum*$^{-/-}$. Both epithelial and stromal thickness are more reduced in *Lum*$^{-/-}$ and *Lum*$^{-/-}$/*Kera-Lum* than in wild type mice. The asterisk indictates significannce ($p<0.05$) versus WT; The hash mark indicates significannce ($p<0.05$) versus *Lum*$^{-/-}$ (ANOVA, Newman-Keuls test).

rior stroma [3-5,17]. In addition, *Lum*$^{-/-}$ mice have reduced corneal keratocan levels [6]. In the present study, we investigated whether reexpression of lumican in the *Lum*$^{-/-}$ cornea could rescue these phenotypic deficits by using *Lum*$^{-/-}$/*Kera-Lum* mice carrying a keratocan promoter-driven lumican transgene [6] in a *Lum*$^{-/-}$ background.

As shown in Figure 1, not only corneal stromal but also epithelial thickness was reduced in *Lum*$^{-/-}$ mice as compared to WT (*Lum*$^{+/+}$ and *Lum*$^{+/-}$ combined) mice. This effect on epithelium was not observed in previous knockout models of CD-1 background [5,8]. The presence of the lumican transgene did not increase either corneal stromal or epithelial thickness to WT levels. Nevertheless, epithelial thickness was increased in *Lum*$^{-/-}$/*Kera-Lum* as compared to *Lum*$^{-/-}$ mice (Figure 1A). The slightly higher stromal thickness in bitransgenic *Lum*$^{-/-}$/*Kera-Lum* corneas did not reach statistical significance (Figure 1B). Corneal opacity was reduced from 1,116±55.2 in the *Lum*$^{-/-}$ mice to 927.6±43.7 in *Lum*$^{-/-}$/*Kera-Lum* mice (Figure 2). Although the latter was still higher than the value in WT mice in this study of 489.1±28.6 units (n=7; not shown), the improvement was significant ($p<0.01$).

Ultrastructural analyses of the corneal stroma demonstrated a remarkable recovery in the fibrillar organization in the posterior stroma of *Lum*$^{-/-}$/*Kera-Lum* compared to *Lum*$^{-/-}$ mice (Figure 3A). The anterior phenotype was comparable to that seen in *Lum*$^{-/-}$ and WT mice. The recovery of the posterior stroma was confirmed after examination of fibril diameter distributions. The number of large-diameter (>40 nm) fibrils was significantly lower ($p=0.0013$, χ^2-test) in *Lum*$^{-/-}$/*Kera-Lum* than in *Lum*$^{-/-}$ mouse posterior stroma (Figure 3B).

Finally, the levels of keratocan protein and message were determined by western blotting and real-time RT-PCR, respectively (Figure 4). On average, the keratocan protein level was increased ($p<0.05$, Welch's *t*-test) in *Lum*$^{-/-}$/*Kera-Lum* as compared to *Lum*$^{-/-}$ mice (Figure 4B) whereas no significant difference was detected at the mRNA level (Figure 4C). It should be noted that even with the different means, the *Lum*$^{-/-}$ and *Lum*$^{-/-}$/*Kera-Lum* groups had similar median keratocan levels (Figure 4B, dotted line), reflecting the broad variation in the *Lum*$^{-/-}$/*Kera-Lum* mice as is also evident when comparing Figure 4A, top row, lanes 1 and 2. A wide variation was not found for keratocan mRNA values, but it should be pointed out that the number of samples for RT-PCR was limited. As shown in Figure 4A, lumican expression was detectable in *Lum*$^{-/-}$/*Kera-Lum* cornea (bottom row, lanes 1 and 2), but overall, the changes were too subtle for accurate quantification. Quantifying changes in keratocan levels was feasible probably because those were amplified.

DISCUSSION

The data presented here demonstrate that reexpression of corneal lumican in a lumican-null background is able to rescue phenotypic deficits. In particular, significant improvements in corneal epithelial thickness, transparency, collagen matrix organization, and keratocan protein levels were observed. However, the *Lum*$^{-/-}$/*Kera-Lum* corneas were still deficient in most of these parameters when compared to WT mice. Furthermore, some other parameters examined were not affected by the lumican transgene at all. The reduced thickness of the corneal stromal layers in *Lum*$^{-/-}$ mice was unchanged in the

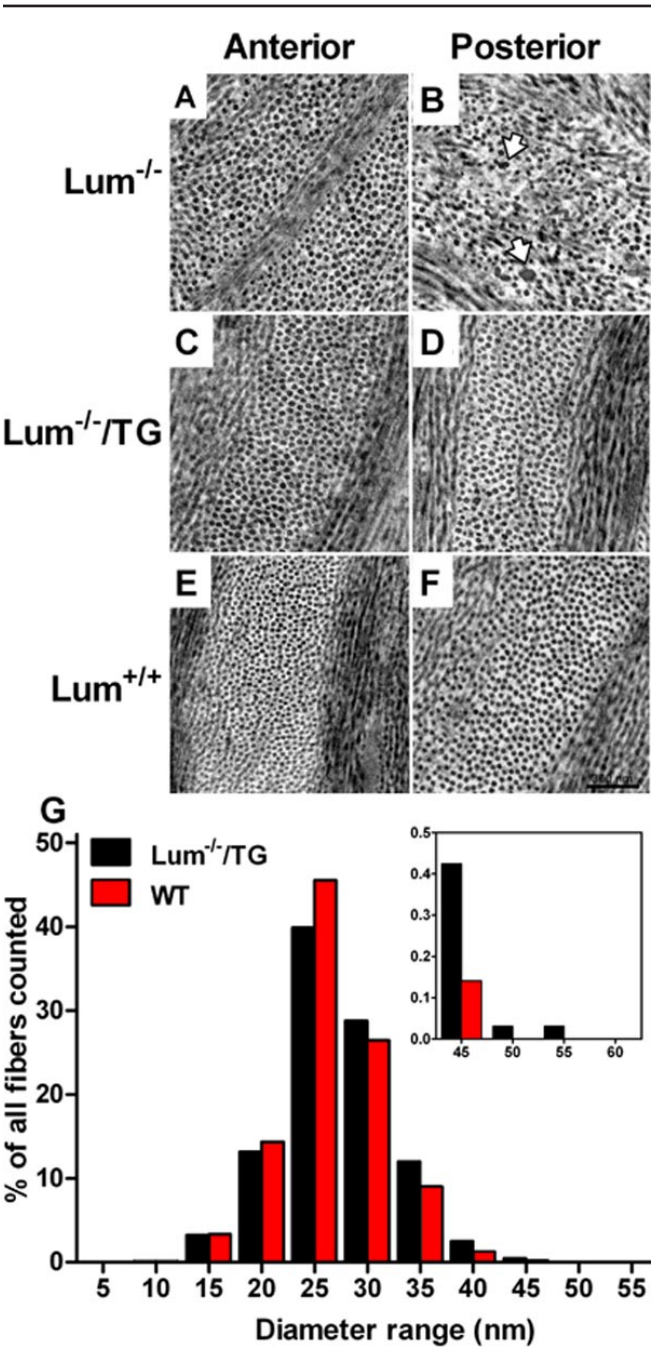

Figure 3. Ultrastructural analysis of stromal collagen matrix organization in corneas from *Lum*$^{-/-}$, *Lum*$^{-/-}$/*Kera-Lum*, and WT mice. After experiments represented in Figure 1 and Figure 2, mouse eyes were processed for transmission EM as described in Methods. **A**-**F**: EM images of anterior stroma (**A**, **C**, **E**) show little difference between groups whereas in EM images of posterior stroma (**B**, **D**, **F**), the matrix in *Lum*$^{-/-}$/*Kera-Lum* (**D**) appears normal like in WT (**F**) and lacks the disarray and large-diameter fibrils (arrows) of *Lum*$^{-/-}$ (**B**). **G**: The distribution of fibril diameters (5 nm bins) in posterior corneal stroma is shown. Inset: frequency of fibrils larger than 40 nm. Data represent percent of 1815, 2224, and 1893 fibrils measured in *Lum*$^{-/-}$, *Lum*$^{-/-}$/*Kera-Lum*, and WT, respectively.

presence of the transgene. Also, no differences in keratocan mRNA expression were detected between *Lum*$^{-/-}$ and *Lum*$^{-/-}$/*Kera-Lum* mice, albeit that there was a two-fold increase in keratocan protein. Thus, the rescue of phenotypic deficits was not complete.

Lumican is present in a wide range of connective tissues, and its absence results in multiple deficiencies [4]. Since it is shown here that the corneal stroma-specific lumican transgene is only partially effective, it can not be absolutely excluded that a systemic lack of lumican may contribute to the corneal deficiencies in *Lum*$^{-/-}$ mice. This notion of indirect actions of lumican is supported by the observation that the corneal epithelium, a tissue that does not contain lumican, is thinner in *Lum*$^{-/-}$ mice of this background strain and was partially rescued by reexpression of lumican in the adjacent stroma in *Lum*$^{-/-}$*/Kera-Lum* mice. It should be noted that previous studies by Chakravarti and associates [5,8] showed no significant difference in corneal epithelium thickness between wild type and *Lum*$^{-/-}$ mice. The different outcomes in epithelium thickness can be explained in part by the dissimilarity in genetic background of the experimental mice. In the present studies, our experimental mice are in a mixed 129/J and C57BL genetic background whereas the *Lum*$^{-/-}$ mice used by Chakravarti et al. [3-5] were in a CD-1 genetic background. In any case, the absence of lumican from surrounding ocular surface tissues such as the periocular mesenchyme and eyelid stroma may have contributed to the incomplete rescue of the corneal phenotype by the solely stromal presence of lumican in *Lum*$^{-/-}$/*Kera-Lum* mice.

On the other hand, low keratocan promoter activity in the *Lum*$^{-/-}$ genetic background as evident from Figure 4 may provide the foremost explanation for the incomplete rescue seen in this study. In a WT background, endogenous keratocan is abundant and as our previous study shows, the *Kera-Lum* transgene induces robust overexpression of lumican as well as keratocan [6]. That same study also showed that keratocan expression is dependent on lumican and that in a *Lum*$^{-/-}$ background, keratocan levels are very low. Therefore, it may be assumed that in the *Lum*$^{-/-}$/*Kera-Lum* mice, transcriptional activity of the *Kera-Lum* transgene is sluggish. Thus, it is likely that low levels of both transgenic lumican and keratocan fail to completely restore corneal morphology and functions.

Aside from the restricted presence and low level of transgenic lumican, another factor contributing to its limited rescue effect could be the developmental timing of its expression. In the WT mouse cornea, lumican is expressed by E12

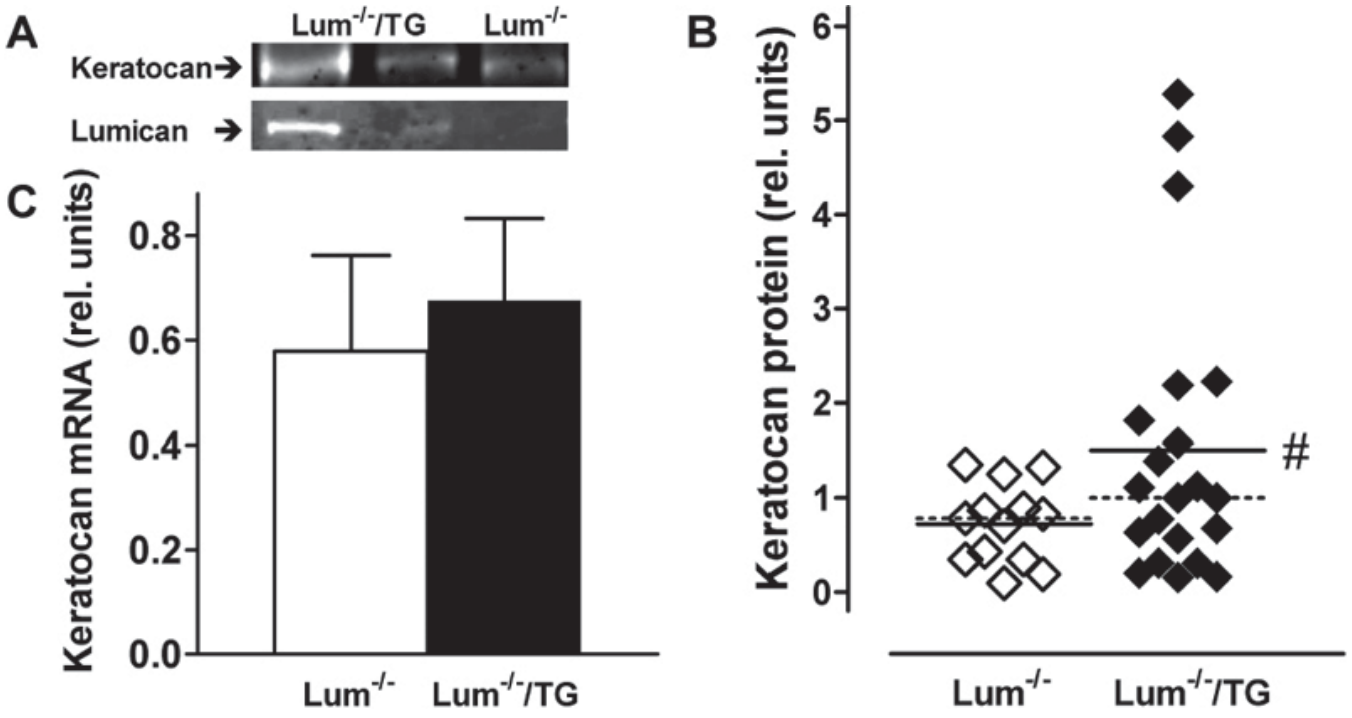

Figure 4. Relative keratocan levels in *Lum*$^{-/-}$ and *Lum*$^{-/-}$/*Kera-Lum* (*Lum*$^{-/-}$/TG) mice. **A**,**B**: After SDS-PAGE/western blotting of cornea extracts, immunopositive bands were visualized on a LI-COR Odyssey Infrared Imaging system. **A**: Examples of keratocan (top row) and lumican (bottom row) protein bands in two *Lum*$^{-/-}$*/Kera-Lum* (left two lanes) and one *Lum*$^{-/-}$ (right lane) cornea. Note the variation in band intensity between the individual *Lum*$^{-/-}$/*Kera-Lum* samples. **B**: Keratocan-immunopositive band intensities were determined and normalized against one *Lum*$^{-/-}$ value. Symbols represent the relative keratocan protein level in each sample (one cornea/mouse), solid lines represent the mean values and the dotted lines represent the medians of 13 *Lum*$^{-/-}$ and 21 *Lum*$^{-/-}$/*Kera-Lum* mice. **C**: From the remaining corneas (one/mouse), RNA was extracted and real-time PCR for keratocan was performed with β-actin as the reference gene. Relative keratocan levels were computed as described in Methods as the ratios over the same *Lum*$^{-/-}$ value. Bars represent mean±SEM of 11 *Lum*$^{-/-}$ mice and 10 *Lum*$^{-/-}$/*Kera-Lum* mice. The hash mark represents the significance ($p<0.05$) versus *Lum*$^{-/-}$ (*t*-test with Welch's correction).

[18] whereas keratocan is detectable and presumably the keratocan promoter is active by E13.5 [19]. Hence, in *Lum*$^{-/-}$/*Kera-Lum* cornea, lumican expression is delayed until E13.5. Moreover, it is conceivable that in a *Lum*$^{-/-}$ background, keratocan is not expressed until well beyond E13.5 due to the absence of endogenous lumican to power up its promoter. It is worthy to mention that there is a surge of keratan sulfate proteoglycan (KSPG) synthesis during neonatal stromal development before eye opening. It has been suggested that such an increase in KSPG synthesis is crucial for a normal growth of stroma [20]. Therefore, a lack of any stromal lumican expression in the proper developmental window (in this case between E12 and at least E13.5) and during the neonatal stages before eye opening may have also hampered a complete rescue of corneal deficiencies.

Regardless of the low initial keratocan promoter activity, if sufficient transgenic lumican accumulated in the *Lum*$^{-/-}$/*Kera-Lum* cornea over time, the activity of *Kera-Lum* transgene might gradually increase thereby further raising transgene and keratocan expression. The outlying values in the measurements of corneal haze and keratocan expression could be interpreted to suggest that such a feed-forward loop was generated in a few cases. Of note, there was no discernible correlation between low corneal haze and high keratocan expression (data not shown). Even so, the outcome of transgenic lumican expression may have differed per eye depending on its intrastromal site of accumulation.

On the whole, it appears that some corneal properties require much earlier and/or higher expression of lumican for their normal function than others. The modest level of lumican expressed by the transgene and the concurrent subtle increase in keratocan expression were enough to restore collagen fibril assembly and matrix organization in the posterior stroma of *Lum*$^{-/-}$/*Kera-Lum* corneas. Normal stromal fibril diameter results from the interaction of fibrils with fibril-associated molecules such as lumican in the posterior stroma. In the absence of lumican, the fibrils associate laterally and give rise to larger diameter fibrils not characteristic of cornea but the norm in tissues like sclera. This lateral fusion disrupts fibril spacing and leads to a less organized posterior stroma. In addition, lumican and other small leucine-rich proteoglycans (SLRPs) may be involved in the regular packing, and thus, the absence of lumican would result in the less ordered packing. In the *Lum*$^{-/-}$/*Kera-Lum* mice, there is apparently sufficient lumican to stabilize the fibrils and prevent lateral association and fusion. Furthermore, the availability of lumican to associate with and organize fibrils may account for the regular packing of the posterior corneal stroma in *Lum*$^{-/-}$/*Kera-Lum* mice. In contrast, corneal thickness and transparency were not raised to wild type levels. This suggests that lumican has multiple mechanisms of action. It has been shown that lumican regulates collagen fibril assembly by direct interaction in the ECM [21]. Furthermore, lumican is able to affect cell function by binding to cell surface receptors [22,23]. Intracellular actions of lumican can also not be excluded.

In summary, the present study shows that reexpression of lumican in the cornea in a *Lum*$^{-/-}$ background only partially rescued corneal phenotypic deficiencies. We propose that the absence of lumican in surrounding tissues, the delay in lumican transgene expression, and/or the low level of its expression are factors contributing to the incomplete recovery. Nonetheless, the lumican transgene resulted in significant improvements in corneal morphology and function.

ACKNOWLEDGEMENTS

This study was supported by NEI EY011845 (W.W.K.), NEI EY005129 (D.E.B.), Research to Prevent Blindness (W.W.K.), Ohio Lions Eye Research Foundation (W.W.K.).

REFERENCES

1. Kao WW, Liu CY. Roles of lumican and keratocan on corneal transparency. Glycoconj J 2002; 19:275-85.
2. Liu CY, Birk DE, Hassell JR, Kane B, Kao WW. Keratocan-deficient mice display alterations in corneal structure. J Biol Chem 2003; 278:21672-7.
3. Saika S, Shiraishi A, Liu CY, Funderburgh JL, Kao CW, Converse RL, Kao WW. Role of lumican in the corneal epithelium during wound healing. J Biol Chem 2000; 275:2607-12.
4. Chakravarti S, Magnuson T, Lass JH, Jepsen KJ, LaMantia C, Carroll H. Lumican regulates collagen fibril assembly: skin fragility and corneal opacity in the absence of lumican. J Cell Biol 1998; 141:1277-86.
5. Chakravarti S, Petroll WM, Hassell JR, Jester JV, Lass JH, Paul J, Birk DE. Corneal opacity in lumican-null mice: defects in collagen fibril structure and packing in the posterior stroma. Invest Ophthalmol Vis Sci 2000; 41:3365-73.
6. Carlson EC, Liu CY, Chikama T, Hayashi Y, Kao CW, Birk DE, Funderburgh JL, Jester JV, Kao WW. Keratocan, a cornea-specific keratan sulfate proteoglycan, is regulated by lumican. J Biol Chem 2005; 280:25541-7.
7. Chakravarti S, Zhang G, Chervoneva I, Roberts L, Birk DE. Collagen fibril assembly during postnatal development and dysfunctional regulation in the lumican-deficient murine cornea. Dev Dyn 2006; 235:2493-506.
8. Jester JV, Ghee Lee Y, Li J, Chakravarti S, Paul J, Petroll WM, Dwight Cavanagh H. Measurement of corneal sublayer thickness and transparency in transgenic mice with altered corneal clarity using in vivo confocal microscopy. Vision Res 2001; 41:1283-90.
9. Li J, Jester JV, Cavanagh HD, Black TD, Petroll WM. On-line 3-dimensional confocal imaging in vivo. Invest Ophthalmol Vis Sci 2000; 41:2945-53.
10. Jester JV, Petroll WM, Cavanagh HD. Measurement of tissue thickness using confocal microscopy. Methods Enzymol 1999; 307:230-45.
11. Li HF, Petroll WM, Moller-Pedersen T, Maurer JK, Cavanagh HD, Jester JV. Epithelial and corneal thickness measurements by in vivo confocal microscopy through focusing (CMTF). Curr Eye Res 1997; 16:214-21.
12. Birk DE, Trelstad RL. Extracellular compartments in matrix morphogenesis: collagen fibril, bundle, and lamellar formation by corneal fibroblasts. J Cell Biol 1984; 99:2024-33.
13. Birk DE, Trelstad RL. Fibroblasts create compartments in the extracellular space where collagen polymerizes into fibrils and fibrils associate into bundles. Ann N Y Acad Sci 1985; 460:258-66.
14. Birk DE, Zycband EI, Winkelmann DA, Trelstad RL. Collagen fibrillogenesis in situ: fibril segments are intermediates in ma-

trix assembly. Proc Natl Acad Sci U S A 1989; 86:4549-53.
15. Pfaffl MW. A new mathematical model for relative quantification in real-time RT-PCR. Nucleic Acids Res 2001; 29:e45.
16. Hayashi Y, Liu CY, Jester JJ, Hayashi M, Wang IJ, Funderburgh JL, Saika S, Roughley PJ, Kao CW, Kao WW. Excess biglycan causes eyelid malformation by perturbing muscle development and TGF-alpha signaling. Dev Biol 2005; 277:222-34.
17. Quantock AJ, Meek KM, Chakravarti S. An x-ray diffraction investigation of corneal structure in lumican-deficient mice. Invest Ophthalmol Vis Sci 2001; 42:1750-6.
18. Ying S, Shiraishi A, Kao CW, Converse RL, Funderburgh JL, Swiergiel J, Roth MR, Conrad GW, Kao WW. Characterization and expression of the mouse lumican gene. J Biol Chem 1997; 272:30306-13.
19. Liu CY, Shiraishi A, Kao CW, Converse RL, Funderburgh JL, Corpuz LM, Conrad GW, Kao WW. The cloning of mouse keratocan cDNA and genomic DNA and the characterization of its expression during eye development. J Biol Chem 1998; 273:22584-8.
20. Song J, Lee YG, Houston J, Petroll WM, Chakravarti S, Cavanagh HD, Jester JV. Neonatal corneal stromal development in the normal and lumican-deficient mouse. Invest Ophthalmol Vis Sci 2003; 44:548-57.
21. Rada JA, Cornuet PK, Hassell JR. Regulation of corneal collagen fibrillogenesis in vitro by corneal proteoglycan (lumican and decorin) core proteins. Exp Eye Res 1993; 56:635-48.
22. Funderburgh JL, Mitschler RR, Funderburgh ML, Roth MR, Chapes SK, Conrad GW. Macrophage receptors for lumican. A corneal keratan sulfate proteoglycan. Invest Ophthalmol Vis Sci 1997; 38:1159-67.
23. Vij N, Roberts L, Joyce S, Chakravarti S. Lumican regulates corneal inflammatory responses by modulating Fas-Fas ligand signaling. Invest Ophthalmol Vis Sci 2005; 46:88-95.

The print version of this article was created on 18 Oct 2007. This reflects all typographical corrections and errata to the article through that date. Details of any changes may be found in the online version of the article.